Forward Kinematics of Cable-driven Continuum Robot Using Optimization

K.P. Ashwin[1] and Ashitava Ghosal[1]

[1]Indian Institute of Science, Bangalore
Email: {ashwinkp, asitava}@iisc.ac.in

Abstract

An elephant trunk robot is continuum robot consisting of a flexible backbone actuated by two pairs of cables (or tendons) offset by a distance and along the circumference of the backbone. By pulling the cables, the continuum robot assumes the shape of an arc of a circle in 3D space. In literature, forward kinematics of the robot has been developed using differential geometry of 3D curves. In this paper, we show that forward kinematics can also be obtained by discretizing along the length of the robot, with each discrete element modelled as a four-bar mechanism, and using a minimization approach. Each of the four-bar mechanism is assumed to be rigid with constant link length. It is shown that minimizing the angle made by the coupler link with the fixed link of the parallel linkage results in a profile which is numerically same as that derived from differential geometry for a segment of cable driven robot in 2D. The results obtained for actuation in 2D is extended to 3D, using two four-bar mechanisms actuated by the two sets of cables, and it is shown to match the analytical formulation available in literature. The proposed method of using a sequence of four-bar mechanisms opens up a new perspective in modelling the forward kinematics of cable driven continuum robots.

Keywords: : elephant trunk robot, flexible robots, four-bar mechanism, 2D and 3D motion

1   Introduction

Continuum robots are generally serial robots which use flexible links instead of rigid links. Since the degree of freedom of such robots are infinite, they possess all the advantages of a hyper-redundant robot. A detailed review on the design, history and applications of continuum robots can be found in [1] and [2]. One of the earliest continuum robot developed was the Rice/Clemson 'elephant-trunk' robot shown in [3] (refer Fig. 1). The robot which resembles a spinal column structure consists of a flexible backbone whose pose can be adjusted by pulling a
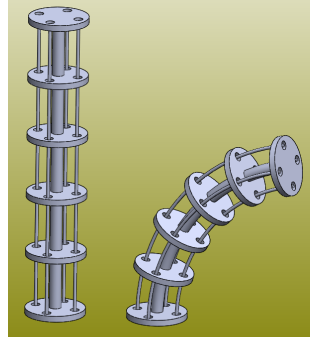
Figure 1: Elephant trunk robot [3]

Figure 2: Elephant trunk robot configuration

set of cables attached to it (refer Fig. 2). The robot is made of multiple segments and each segment can be actuated using a set of four cables which are placed 90° apart from each other. Guide disk attached at regular intervals on the backbone routes the cables (tendons) from the base of the robot till the tip of the segment so that the separation between the cables are maintained. Detailed analysis of the workspace of the robot can be found in reference [4]. Many advanced flexible robots are modifications of this original concept, with difference mostly in the actuation mechanism (see [5] and [6]).

The forward kinematics of the cable driven continuum robot is to find the pose of the robot when the lengths of cables are given. In reference [7] Gravagne and Walker derived analytical expressions for the forward kinematics of elephant trunk robot using concepts from differential geometry. The co-ordinates of a point on the robot is determined using two parameters—α which is angle of rotation of the plane that contains the final configuration of the robot and about the initial axis of the robot[1] and the angle $\beta(s)$ made by the tangent of backbone with the initial axis (which varies along the length of the deformed backbone). In this paper, we show that the forward kinematics solutions derived in the literature can also be obtained by solving an optimization problem. While extending the differential geometry based analytical methods to solve the model could be non-trivial for uneven spacing between the cables and for robots with general cable routing, the method proposed in this paper could provide a simpler alternative for tackling such complexities. In section 2, the forward kinematics model for single cable actuation and the resulting configuration in 2D plane is discussed. Extension of the method to out-of-plane bending of the actuator is shown in section 3. Finally, conclusions are presented in section 4

---

[1]The configuration of the robot will always be in a plane and is shown to take the shape of an arc of a circle.
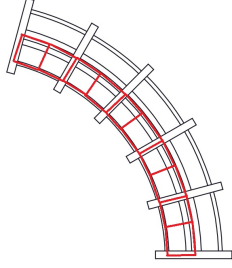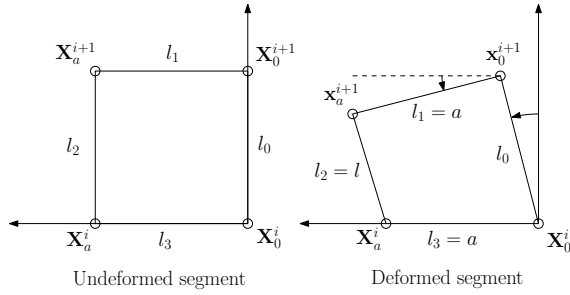
Figure 3: Discretization of robot in 2D plane

Figure 4: Nomenclature for single segment

2 Forward Kinematics Model for 2D Continuum Robot

In a cable driven continuum robot with two pairs of cables, if the two opposing cables in one of the pairs (cables which are 180° apart) are actuated, the robot will be restricted to move within a 2D plane. Among the opposing cable duo, only one cable is pulled at a time, since otherwise, the robot simply buckles. In this section, the formulation of forward kinematics of 2D planar continuum robot is discussed.

The proposed formulation assumes the profile of the continuum robot as a set of connected 4 bar parallel linkages. To this end, the robot is discretized into n number of segments along the backbone of the continuum robot as shown in Fig. 3. In this approach, only one cable from the opposing cable pair is considered, as it can be seen in the later part of the section that the other cable does not have any role in manipulation of the robot in the quadrants containing the actuated cable[2]. With reference to Fig. 4, one segment of the continuum robot can be approximated as a 4-bar linkage, with the first crank, coupler, second crank and fixed link having lengths l_0, l_1, l_2 and l_3 respectively. Since the cables pass through holes present in the guide disks, the lengths $l_1 = l_3 = a$ where a is the constant spacing between the backbone and the cables. For the robot of length L_0 measured along the backbone, the length of the first crank $l_0 = \dfrac{L_0}{n}$. When the cables are actuated to a final length of $L_a = L_0 - \Delta L_a$ where ΔL_a is the prescribed change in length of the cable, the length of second crank, $l_2 = l = \dfrac{L_a}{n}$. From the loop-closure constraint equations of the 4-bar linkage located at the base of continuum robot, we get

$$f(\theta, \beta) = l_0^2 + 2a^2 - l^2 + 2al_0 \sin(\theta - \beta) - 2a(l_0 \sin \theta + a \cos \beta) = 0 \qquad (1)$$

---

[2]The opposing cable is practically used to retract the robot to its original position if the backbone material is not perfectly elastic, and obviously, for manipulation in the opposing direction of the first cable.
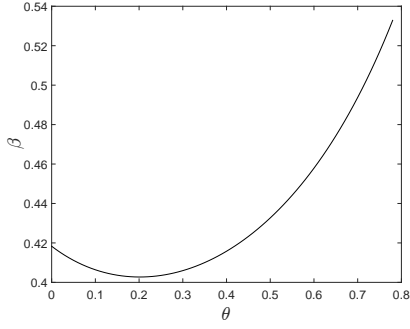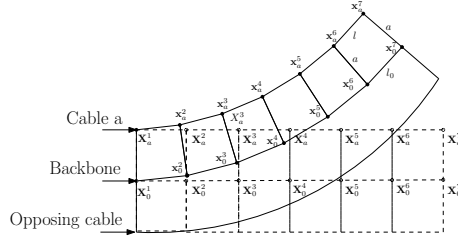
Figure 5: β vs θ

Figure 6: Assembly of 4 bar linkages for iteration procedure

where θ is the angle made by the first crank and the axis of backbone while β is the coupler angle measured relative to the fixed link. Plotting the values of θ and β, we can see from Fig. 5 that a minimum exists for $\beta - \theta$ curve for a given set of length parameters.

Differentiating the above equation with respect to θ and setting $\dfrac{d\beta}{d\theta} = 0$ and simplifying, we get

$$\cos(\theta - \beta) = \cos\theta$$

From the above equation, we can get the value of crank angle (and subsequently a configuration of the linkage) where the rate of change of coupler angle with respect to the crank angle is zero. This is given by

$$\beta = 2(\theta - k\pi) \tag{2}$$

where k is an integer.

In the initial un-actuated configuration, the lengths of link are $l_0 = l_2 = \dfrac{L_0}{n}$. In this position, the initial coupler angle is zero. After actuation, the nearest minimum for the coupler angle (from zero value) appears when $k = 0$, or $\beta = 2\theta$ for small displacements of the first crank. In what follows, it is shown that the configuration which produces minimum change of coupler angle is the same as the configuration obtained analytically by Gravagne and Walker [7].

Substituting $\theta = \dfrac{\beta}{2}$ in Eq. (1) and simplifying, we get

$$-l^2 + \left(l_0 - 2a\sin\left(\frac{\beta}{2}\right)\right)^2 = 0 \tag{3}$$

Since l takes only positive values, we get

$$\sin\frac{\beta}{2} = \frac{l_0 - l}{2a} \tag{4}$$

4

The assembled discrete segments represent the robotic continuum for large values of n. In that case, the right-hand side of the above equation will be very small. For small angles, we get

$$\beta = \frac{l_0 - l}{a} \tag{5}$$

The value of coupler angle for the distal tip, which is same as the angle $\beta(L_0)$ in the derivation shown in [7], can be found by multiplying the above expression for β with the total number of segments n. The value of coupler angle so obtained,

$$\beta(L_0) = n\frac{l_0 - l}{a} = \frac{\Delta L_a}{a} \tag{6}$$

is same as the value obtained analytically in [7].

Since it has been shown that the forward kinematics of continuum robot can be obtained by minimizing the coupler angle of approximated 4 bar parallel linkages, the following formulation may be used to easily implement the optimization procedure:

The co-ordinates of the ends of the coupler attached to the first crank and the second crank in the undeformed position are given by $\mathbf{X}_0^{i+1}$ and $\mathbf{X}_a^{i+1}$, respectively. The corresponding deformed positions will be $\mathbf{x}_0^{i+1}$ and $\mathbf{x}_a^{i+1}$, respectively. Similarly, the co-ordinates of the ends of the fixed link attached to the first crank and the second crank are given by $\mathbf{X}_0^i$ and $\mathbf{X}_a^i$, respectively. For the segment at the base of robot $i = 1$ and $i = n$ at the tip. With the above, the optimization problem may be formulated as:

$$\underset{\mathbf{x}_b^{i+1}, \mathbf{x}_a^{i+1}}{\arg\min} \quad \arccos\left(\left(\frac{\mathbf{X}_0^i - \mathbf{X}_a^i}{\|\mathbf{X}_0^i - \mathbf{X}_a^i\|}\right) \cdot \left(\frac{\mathbf{x}_0^{i+1} - \mathbf{x}_a^{i+1}}{\|\mathbf{x}_0^{i+1} - \mathbf{x}_a^{i+1}\|}\right)\right)$$

Subject to:

$$\begin{aligned}
\|\mathbf{x}_0^{i+1} - \mathbf{X}_0^i\| &= l_0 \\
\|\mathbf{x}_a^{i+1} - \mathbf{X}_a^i\| &= l \\
\|\mathbf{x}_0^{i+1} - \mathbf{x}_a^{i+1}\| &= a
\end{aligned} \tag{7}$$

Given: $\mathbf{X}_0^i, \mathbf{X}_0^{i+1}, \mathbf{X}_a^i, \mathbf{X}_a^{i+1}, l_0, l, a$

The solution to the above optimization problem gives the co-ordinates of tips $\mathbf{x}_0^{i+1}$ and $\mathbf{x}_a^{i+1}$ and the iterative method starts from the base segment and proceeds towards the tip of the robot. With reference to Eq. (4), in order to ensure that the right-hand side of the equation is always less than 1, the value of n may be chosen such that

$$n > \frac{L_0 - L_a}{2a} \tag{8}$$

Fig. 7 shows the profile plotted for a continuum robot using the solution obtained from analytical method as well as the discretized optimization method. The solution, as proved before, is exact except for the tolerances in the numerical
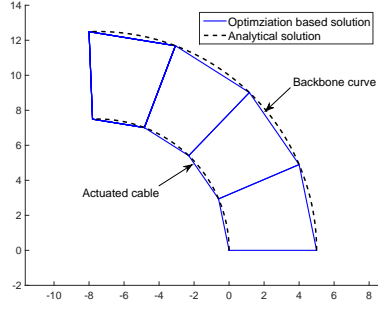
Figure 7: Comparison between analytical and optimization based solutions
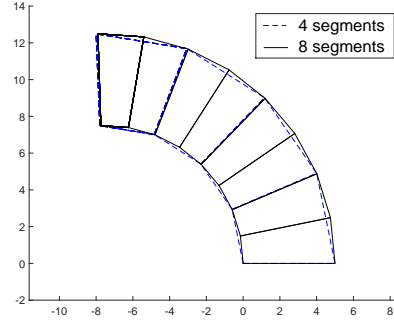

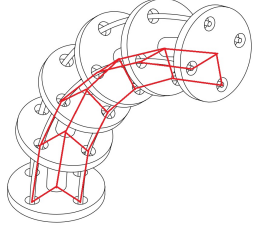Figure 8: Solution with increased number of segments

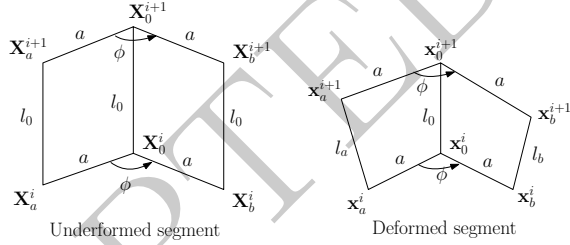Figure 9: Discretization of robot in 3D

Figure 10: Nomenclature of segment in 3D

procedure. Fig. 8 shows that the profile remains unaltered with different number of segments.

In the next section, we extend the approach to 3D continuum robots.

3   Forward Kinematics Model for Continuum Robot in 3D

If both pairs of cables are actuated simultaneously, the continuum robot will assume a deformed pose in 3D space. For simultaneous actuation, the discretization of robot is carried out as shown in Fig.9. Here, the backbone along with the actuating cables which are placed at an angle $\phi = 90°$ apart can be considered as a set of two adjoined 4 bar linkages (a 7-bar linkage). The two quadrilaterals have the vertices $\left(\mathbf{X}_0^i, \mathbf{X}_0^{i+1}, \mathbf{X}_a^{i+1}, \mathbf{X}_a^i\right)$ and $\left(\mathbf{X}_0^i, \mathbf{X}_0^{i+1}, \mathbf{X}_b^{i+1}, \mathbf{X}_b^i\right)$ initially. These quantities change to $\left(\mathbf{X}_0^i, \mathbf{x}_0^{i+1}, \mathbf{x}_a^{i+1}, \mathbf{X}_a^i\right)$ and $\left(\mathbf{X}_0^i, \mathbf{x}_0^{i+1}, \mathbf{x}_b^{i+1}, \mathbf{X}_b^i\right)$ after actuation. The subscripts a and b are used to denote the respective values for the linkages formed by cable pairs a and b respectively. The coupler angles may be defined as β_a and β_b for the two 4-bar linkages.

6

Since the deformation of the robot is commutative– i.e., the actuation is the same irrespective of the order of actuating the cables, the final pose will be the one where coupler angles of both the linkages are minimized simultaneously and independently. Hence, the pose can be determined from solving the optimization problem

$$\underset{\mathbf{x}_b^{i+1},\mathbf{x}_a^{i+1}}{\arg\min} \quad \left[\arccos\left(\left(\frac{\mathbf{X}_0^i - \mathbf{X}_a^i}{\|\mathbf{X}_0^i - \mathbf{X}_a^i\|}\right) \cdot \left(\frac{\mathbf{x}_0^{i+1} - \mathbf{x}_a^{i+1}}{\|\mathbf{x}_0^{i+1} - \mathbf{x}_a^{i+1}\|}\right)\right)\right]^2 + \tag{9}$$

$$\left[\arccos\left(\left(\frac{\mathbf{X}_0^i - \mathbf{X}_b^i}{\|\mathbf{X}_0^i - \mathbf{X}_b^i\|}\right) \cdot \left(\frac{\mathbf{x}_0^{i+1} - \mathbf{x}_b^{i+1}}{\|\mathbf{x}_0^{i+1} - \mathbf{x}_b^{i+1}\|}\right)\right)\right]^2$$

Subject to:

$$\|\mathbf{x}_0^{i+1} - \mathbf{X}_0^i\| = l_0 \tag{10}$$
$$\|\mathbf{x}_a^{i+1} - \mathbf{X}_a^i\| = l_a$$
$$\|\mathbf{x}_b^{i+1} - \mathbf{X}_b^i\| = l_b$$
$$\|\mathbf{x}_0^{i+1} - \mathbf{x}_a^{i+1}\| = a$$
$$\|\mathbf{x}_0^{i+1} - \mathbf{x}_b^{i+1}\| = a$$
$$\arccos\left(\left(\frac{\mathbf{x}_0^i - \mathbf{x}_a^i}{\|\mathbf{x}_0^i - \mathbf{x}_a^i\|}\right) \cdot \left(\frac{\mathbf{x}_0^i - \mathbf{x}_b^i}{\|\mathbf{x}_0^i - \mathbf{x}_b^i\|}\right)\right) - \arccos\left(\left(\frac{\mathbf{X}_0^i - \mathbf{X}_a^i}{\|\mathbf{X}_0^i - \mathbf{X}_a^i\|}\right) \cdot \left(\frac{\mathbf{X}_0^i - \mathbf{X}_b^i}{\|\mathbf{X}_0^i - \mathbf{X}_b^i\|}\right)\right) = 0$$

Given: $\mathbf{X}_0^i, \mathbf{X}_0^{i+1}, \mathbf{X}_a^i, \mathbf{X}_a^{i+1}, \mathbf{X}_b^i, \mathbf{X}_b^{i+1}, l_0, l_a, l_b, a$

where $l_a = \dfrac{L_a}{n}$, $l_b = \dfrac{L_b}{n}$ and the last equality constraint ensures that the separation between the cables remains constant even after deformation.

In Fig. 11 and Fig. 12, the pose of robot with two cables actuated by equal amounts as well as by different values are shown. As is the case with the 2D, analytical solution and optimization based solution varies only by the numerical error induced due to the optimization scheme.

To summarize, it is shown that the forward kinematics of a cable-driven continuum robot, with a fixed tendon spacing can be calculated using an optimization based approach. Here, the actuating cable of the continuum robot as well as the backbone are discretized to a number of segments and the two are considered as the two cranks of a 4-bar linkage. The constant spacing between the cable and the backbone separates the cranks and form the fixed link as well as the coupler. Minimizing the coupler angle from the stationary initial position based on the constraints imposed by the cable lengths, backbone length as well as the constant spacing between the cable and backbone, a unique pose is obtained for the robot, which is shown to match the solution obtained using differential geometric approach.

It is worth noting that the approach is applicable only if the given lengths are constant. i.e, for example, for a robot which does not have guiding disks to keep a constant cable spacing will result in varying values for 'a' and this approach may not be used in the present form. For the case where the cables are passed
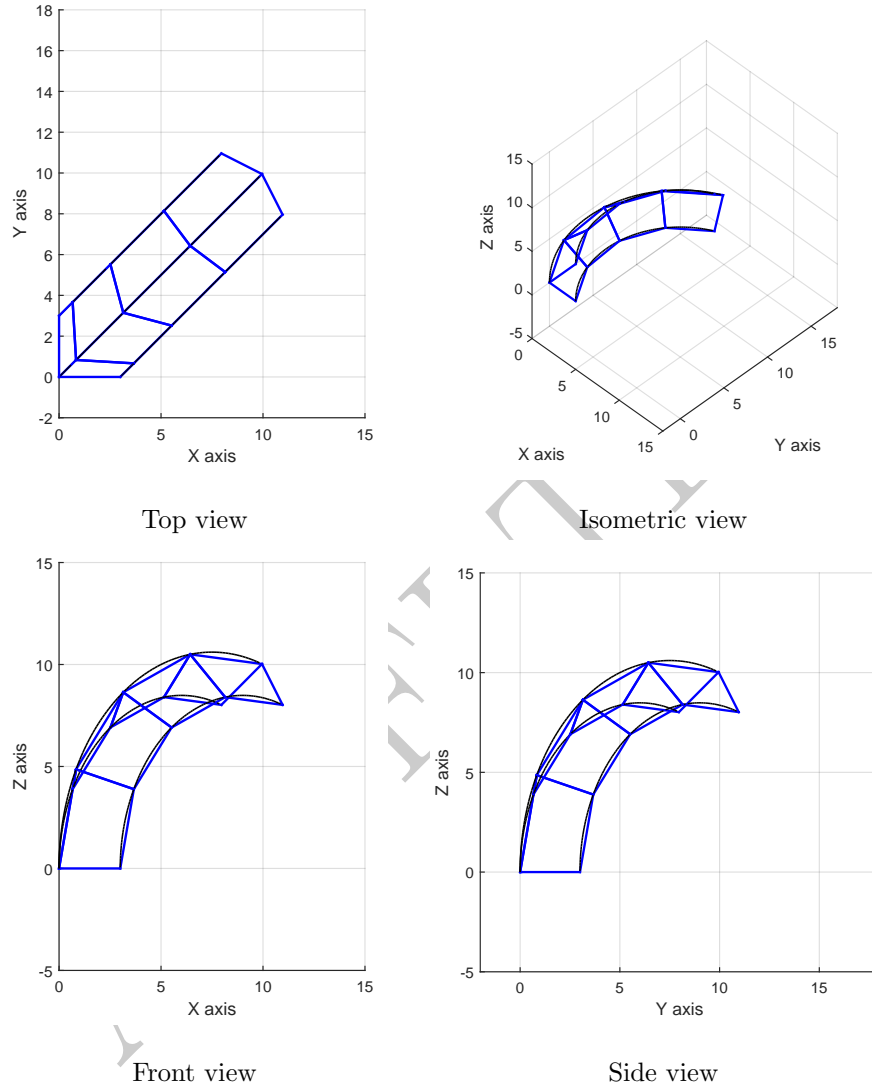
Figure 11: Profile of robot with cables actuated by equal displacements. (Black lines for analytical solution and blue lines for optimization based solution)
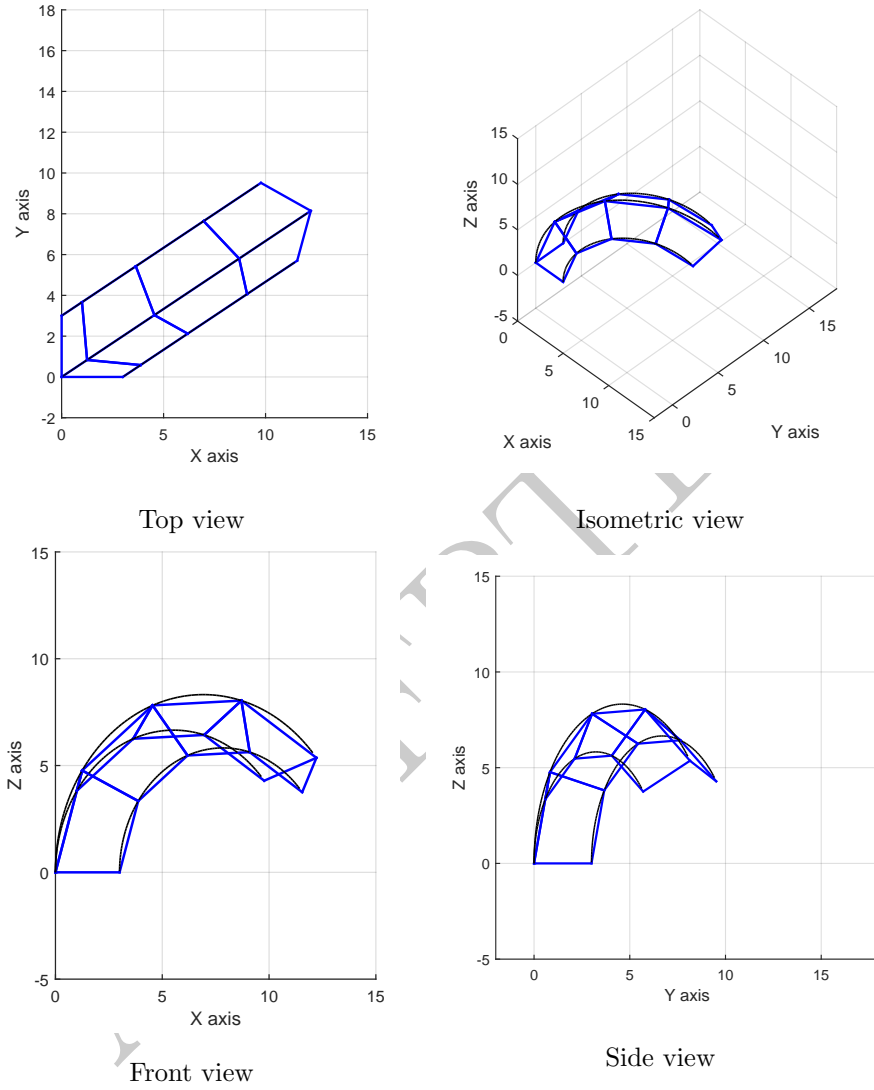
Figure 12: Profile of robot with cables actuated by different displacements. (Black lines for analytical solution and blue lines for optimization based solution)

through guiding disks with holes drilled with different spacings, the cables will not drift in circumferential direction. In reference [8], forward kinematics of such a system with general tendon routing is posed using a set of differential equations based on Cosserat theory. However, the expressions are clearly non-intuitive and are applicable to tendon routes that can be analytically expressed. Meanwhile, in the optimization based method proposed in this paper, the same would translate to adding specific constraints to the problem, such as:

$$\|\mathbf{x}_0^{i+1} - \mathbf{x}_a^{i+1}\|_j = a_j \tag{11}$$

$$\|\mathbf{x}_0^{i+1} - \mathbf{x}_b^{i+1}\|_j = a_j \tag{12}$$

$$\left\{ \arccos\left(\left(\frac{\mathbf{x}_0^i - \mathbf{x}_a^i}{\|\mathbf{x}_0^i - \mathbf{x}_a^i\|}\right) \cdot \left(\frac{\mathbf{x}_0^i - \mathbf{x}_b^i}{\|\mathbf{x}_0^i - \mathbf{x}_b^i\|}\right)\right) - \right. \tag{13}$$

$$\left. \arccos\left(\left(\frac{\mathbf{X}_0^i - \mathbf{X}_a^i}{\|\mathbf{X}_0^i - \mathbf{X}_a^i\|}\right) \cdot \left(\frac{\mathbf{X}_0^i - \mathbf{X}_b^i}{\|\mathbf{X}_0^i - \mathbf{X}_b^i\|}\right)\right) \right\}_j = \phi_j \tag{14}$$

where $(\cdot)_j$ represent the specified values at segment index j. The validity of this claim is however, yet to be confirmed with detailed experiments.

4   Conclusions

The forward kinematics of cable driven continuum robots such as the well-known Rice/Clemson elephant trunk has been analytically solved by Gravagne and Walker based on differential geometry. It is shown in this paper that the same can also be achieved using optimization methods. The continuum robot is discretized into segments with each segment represented as a 4-bar parallelogram linkage for planar manipulation. From the initial horizontal position of the coupler, a unique pose of the 4-bar linkage is obtained by minimizing the angle made by coupler with the fixed link, while maintaining the constraints of link lengths. When the iterative process is continued for the entire robot, the resulting pose is shown to be the same as the one derived using the traditional differential geometric methods. A minimum number of segments required for the procedure is also suggested based on the derivation and the method shows consistency with varying number of segments. The concept is directly extended to 3D using a 7-bar linkage which is basically two adjoined 4-bar linkages. Here, an extra constraint is added for the minimization problem so as to maintain the constant angle between the cables. The numerical procedure and analytical solution are shown to match each other as is the case for 2D.

The method suggested in this paper suggests a new perspective in modelling the forward kinematics of cable driven continuum robots. As one can see, it is easy to apply the modelling technique to robots having uneven separation between the cables and also for robots with generalized cable routing—for which analytical methods could be a daunting task. Research work exploring these areas is ongoing.

References

[1] I. D. Walker, "Continuous backbone 'continuum' robot manipulators," *ISRN Robotics*, vol. 2013, pp. 19, 2013.

[2] G. Robinson, J. B. C. Davies, "Continuum robots-a state of the art," in *Proc. 1999 IEEE Int. Conf. Robotics and Automation*, pp. 2849–2854, 1999.

[3] I. D. Walker, M. W. Hannan, "A novel 'elephant's trunk' robot," in *Proc. IEEE/ASME Int. Conf. Adv. Intel. Mechatronics*, pp. 410–415, 1999.

[4] K. Cao, R. Kang, J. Wang, Z. Song, J. Dai, "Kinematic model and workspace analysis of tendon-driven continuum robots," in *Proc. 14th IFToMM Wold Congress*, pp. 640–644, 2015.

[5] Festo Didactic Inc., 607 Industrial Way West, Eaton-580 town N.J. 07724, www.festo.com, accessed: 2018-06-23.

[6] K. Xu, N. Simaan, "An investigation of the intrinsic force sensing capabilities of continuum robots," *IEEE. Trans. Robotics*, vol. 24(3), pp. 576–587, 2008.

[7] I. A. Gravagne, I. D. Walker, "On the kinematics of remotely-actuated continuum robots," in *Proc. IEEE Intl. Conf. Rob. Aut.*, pp. 2544–2550, 2000.

[8] D. C. Rucker, R. J. Webster III, "Statics and dynamics of continuum robots with general tendon routing and external loading," *IEEE. Trans. Robotics*, vol. 27(6), pp. 1033–1044, 2011.